令　和　五　年　度　　修　士　論　文

Advanced In-Situ Observation Techniques for PBW Micro-machining:Utilizing Ion Beam-Induced Luminescence Analysis and Image Processing Methods

指導教員　　花泉 教授
加田　准教授

群馬大学大学院理工学府 理工学専攻
電子情報・数理教育プログラム
張 錦汕

1Abstract

With the deepening advancements in micro-nanoscale technology, Proton/Particle Beam Writing (PBW) and Ion Beam Induced Luminescence (IBIL) have increasingly become focal points of research. PBW, celebrated for its exceptional performance in high aspect ratio micro-fabrication, has always posed a bottleneck challenge in the engineering realm – real-time monitoring and evaluation during the processing phase. For many manufacturers and researchers, discerning the success or failure of the process in real-time is not just a technological hurdle, but also a matter of production efficiency and cost considerations.

To address this challenge, we initiated this study with a clear objective: to monitor PBW processing in real-time, subsequently reducing unnecessary fabrication costs and enhancing production efficiency. In terms of methodology, by integrating a high-speed wavelength-dispersive IBIL photon counting detector, we meticulously devised our experimental protocol. Employing specialized equipment, we measured IBIL from the focused beam irradiation area across a wavelength range of 320-750 nm. This pioneering effort granted us invaluable experimental data, leading to the successful development of a device that utilizes IBIL technology in real-time during PBW processing. This means, beyond just data acquisition, we are now equipped to

provide clear, high-resolution live images, effectively overseeing the fabrication process.

Moreover, to ensure the clarity of the images captured, we've developed a series of noise reduction algorithms. These algorithms, while substantially enhancing image clarity, also fortify their reliability in practical applications. Through our research, the future of micro-fabrication promises more efficient and precise real-time monitoring, further propelling technological innovation and progress in the entire sector.

2.Introduction

Exploration of the Ion Beam Induced Luminescence Analysis (IBIL) Methodology: Its Research Context and Significance

Ion Beam Induced Luminescence Analysis (IBIL) stands as a non-destructive, sophisticated examination technique, employed to delineate the optical attributes of various materials. This process leverages high-energy ion beams to incite the luminescent characteristics of materials. Since its inception in the 1960s, IBIL has progressively emerged as an integral method for probing the luminescent behaviors of materials, evaluating the performance of optoelectronic devices, and identifying defect structures. With relentless enhancements and breakthroughs in ion beam technology, IBIL has realized significant strides in the characterization of a vast array of materials and performance studies of devices. This overview delves into the research backdrop of the Ion Beam Induced Luminescence Analysis technique, touching upon its governing principles, evolution chronology, realms of application, and future trajectory.

2.1 Governing Principle of the IBIL Methodology

The cornerstone principle underpinning IBIL (Ion Beam Induced Luminescence) technology involves the injection of a high-energy ion

beam into a selected material. This process stimulates the electrons and defects within the material, instigating electron transitions and energy level recombinations, culminating in the generation of photoluminescence. As the high-energy ion beam infiltrates the material, intricate interactions transpire between the ions and the atomic constituents of the material. These interactions yield an abundance of charge carriers that emit photons during the carrier recombination process. These photons, carrying invaluable information about the material's internal energy level structure and defect states, can be detected and analyzed. Given the formidable energy of the ion beam and its exceptional spatial focusing precision, IBIL technology facilitates the non-destructive analysis of specific zones within the material, delivering outstanding spatial resolution and sensitivity.[1][2]

2.1.2 Evolutionary Path of IBIL Technology

The nascent stages of Ion Beam Induced Luminescence (IBIL) technology can be traced back to the early 1960s. During this time, researchers embarked on the utilization of high-energy ion beams to stimulate the photoluminescent traits of semiconductor materials. The ensuing years witnessed continual refinements in ion beam technology, accompanied by leaps in instrumentation sophistication, thereby fueling

the rapid progression of IBIL technology.

As the technology journeyed into the 1980s, the application landscape of IBIL broadened, incorporating a wider range of materials, inclusive of phosphors, quantum dots, and materials doped with rare-earth elements. Concomitantly, the scientific community proposed more efficient methodologies of ion beam excitation, such as electron excitation and electron beam excitation, aimed at boosting the sensitivity and resolution of IBIL technology.

Transitioning into the 21st century, the advent of nanotechnology presented a plethora of opportunities for IBIL technology. It began to find extensive application in the exploration of nanomaterials and nanodevices, providing vital reinforcement for the advancement of nanoscale optoelectronics.

2.1.3 Application Domains of IBIL Technology

Ion Beam Induced Luminescence (IBIL) technology exhibits extensive applicability in the realm of materials science and the fabrication of optoelectronic devices. The first notable application involves the exploration of photoluminescence behavior and defect structure within semiconductor materials, elucidating the correlation between optical properties and electrical performance of these materials.

Moreover, IBIL technology demonstrates remarkable potential in the

study of luminescent materials, including quantum dots, fluorophores, and materials doped with rare-earth elements. Through the application of IBIL technology, researchers can delve deeper into the luminescence mechanisms and performance characteristics of these materials, providing invaluable references for the preparation and implementation of optoelectronic devices.

Additionally, IBIL technology can be utilized for non-destructive testing and performance optimization of optoelectronic devices, delivering indispensable technical assistance for device research, development, and production.

2.1.4 Future Perspectives of Ion Beam Induced Luminescence (IBIL) Technology

In light of the incessant evolution of ion beam technology and materials science, IBIL technology is poised for expanding its application territories and relentlessly enhancing and optimizing its performance. In the future, it is anticipated that IBIL technology will achieve superior spatial resolution and heightened sensitivity, amplifying its applicability in the research of nanoscale materials and devices.

Furthermore, as ion beam technology continues its trajectory of advancement, IBIL technology is envisioned to be integrated with other characterization and processing methodologies, providing a more

comprehensive and diverse arsenal for research in materials science and nanotechnology.

Ultimately, IBIL technology is expected to cement its position as a pivotal instrument and impetus in the research and applications in nanophotonics, catalyzing novel breakthroughs in the development and application of optoelectronic devices.

2.2Proton Beam Writing (PBW) Technology

The Proton/Particle Beam Writing (PBW) technology is a distinctive quantum beam microfabrication technique known for its high selectivity towards the target material and the capability to achieve a high aspect ratio in processing. Up to now, it has been applied to the microfabrication of polymer materials [3,4] and defect engineering of wide bandgap semiconductor materials [5,6].By utilizing high-energy proton beams to deposit energy directly within materials, PBW technology can induce tiny volume changes, enabling high-resolution micrometer to nanometer scale structuring. Over the past few decades, PBW technology has been continuously researched and developed, demonstrating wide application prospects in fields such as nanoscale device manufacturing, photonics devices, and quantum information processing.[7]

2.2.2. Basic Principles of Proton Beam Writing

The fundamental principle of PBW technology is to achieve micro and nanoscale structuring by controlling the energy deposition of high-energy proton beams within materials. When high-energy proton beams enter a material, they interact with the material's atoms, causing ionization and excitation and resulting in energy loss inside the material. The control of proton beam energy and dose can alter the interaction process between the proton beam and the material, leading to the formation of different electronic excitation states and ion beam radiation damage regions within the material. The formation of these radiation damage regions causes volume changes in the material, thus achieving high-resolution micrometer to nanometer scale structuring.

2.2.3 Application Areas of Proton Beam Writing Technology

PBW technology holds wide application prospects in micro and nanodevice manufacturing and photonics device fields. One major application area is in the fabrication of nanophotonics devices. PBW technology can be used to create high-resolution 3D structures, such as micro photonic crystals, optical waveguides, and metamaterials, which play critical roles in nanophotonics devices. Additionally, PBW

technology can be applied to manufacture micro-optics lenses, optical antennas, and micro photonic integrated circuits, providing novel design and fabrication methods for photonics devices.

Another important application area is the development of quantum information processing devices. In the field of quantum information processing, micro and nanoscale structures are crucial for the manipulation and entanglement of quantum bits (qubits). PBW technology's high resolution and 3D processing capabilities make it an ideal choice for manufacturing quantum bits. In recent years, many research institutions have begun exploring the use of PBW technology in manufacturing qubits and quantum communication devices, achieving a series of meaningful advancements.

Furthermore, PBW technology can find applications in other fields, such as biomedical device manufacturing, photonic crystal nanofabrication, and photonic crystal sensors. Its high resolution and controllable characteristics offer new perspectives and solutions for research in these areas.

2.2.4 Development Trends and Challenges of Proton Beam Writing Technology

As nanotechnology rapidly advances, PBW technology continues to

attract attention from researchers and has made significant progress in various fields. However, PBW technology still faces certain challenges. One of them is the issue of processing efficiency and cost. As controlling and injecting proton beams require substantial energy and equipment, PBW technology may encounter higher costs and processing times in practical applications. Therefore, improving the processing efficiency and reducing costs of PBW technology is an urgent problem to address.[8]

Furthermore, the spatial resolution of PBW technology is an aspect that requires further improvement. Although PBW technology already possesses high spatial resolution, certain special materials or structures may demand even higher resolution to meet practical requirements. Hence, enhancing the spatial resolution of PBW technology is an important direction for future research.

2.3Research Question

The purpose of this comprehensive research is to forge a symbiotic union between Proton/Particle Beam Writing (PBW) technology and Ion Beam Induced Luminescence (IBIL) technology. The principle objective of this synergy is to facilitate precise scrutiny and evaluation of material states throughout the intricate processes of micro-fabrication.

Proton/Particle Beam Writing represents a groundbreaking quantum beam-based micro-fabrication technology. Its signature attributes

encompass a notable selectivity towards processing targets and the proficiency to create structures with high aspect ratios. Despite its successful deployment in micro-processing of polymeric materials and defect engineering of wide bandgap semiconductor materials, the necessity for swift understanding of irradiation conditions and diversification of target materials remains imperative for the further refinement of PBW technology.

In this technological landscape, Ion Beam Induced Luminescence (IBIL), a technology adept at analyzing signals reflecting compounds or chemical bonding states via low-energy photons, has emerged as a focal point of interest. This study endeavours to capitalize on the potential of IBIL spectroscopic analysis in a system using MeV-grade focused proton beam irradiation. The ultimate aspiration is to manifest visualization of the target area during or subsequent to PBW irradiation.

In a typical PBW process, the procedural steps include pre-irradiation treatment, PBW irradiation, post-irradiation treatment, culminating in ultraviolet exposure. The success of these procedural steps translates into successful fabrication, a conclusion reached by observing the phosphatic glass under ultraviolet exposure. However, the traditional PBW technology creates a 'black box' scenario post-irradiation, rendering the judgement of fabrication success or failure a daunting task.

The intention, therefore, is to innovate a technology capable of

discerning the success of the fabrication during the PBW process itself. The realization of this capability is projected to contribute significantly towards reducing the overall fabrication duration. The technology under development aims to analyze particles secondary to ion beams, an operation synonymous with Ion Beam Analysis (IBA). The primary interest lies in secondary photons, with the goal of acquiring information pertaining to the chemical form, thus signifying the application of IBIL technology.

It has been observed that IBIL profoundly influences the visualization of irradiation effects in select organic and inorganic substances. The research anticipates that with the inclusion of IBIL, the visualization of the target area during or post-PBW irradiation will be attainable. This advancement signifies a notable breakthrough, as early determination of the success or failure of fabrication is expected to accrue substantial savings in terms of cost and time, aligning with the core objective of the research and exemplifying the transformative potential of the integrated PBW and IBIL technologies in micro-fabrication processes.

3Experimental equipment and methods

3.1Experimental equipment

In the preceding discourse, our research objective is to incorporate IBIL (Induced Beam-Induced Luminescence) detection into the PBW (Particle Beam Writing) process. To realize this, we have fabricated a novel apparatus intended for managing the acquired data.

This apparatus constitutes a sophisticated micro-spectroscopy system. [9]Its operation proceeds as follows: initially, the apparatus receives photons emanating from the workpiece undergoing processing; subsequently, an internal spectroscope within the apparatus guides these photons, segregated by wavelength, to their respective photomultiplier tubes (PMTs). The PMTs tally the photon count, converting this data into a voltage reading that is fed into a Field-Programmable Gate Array (FPGA) circuit for counting. Finally, from this data, we can infer the quantity of photons and their spatial positional information. This elucidates the basic operation cycle of our apparatus.

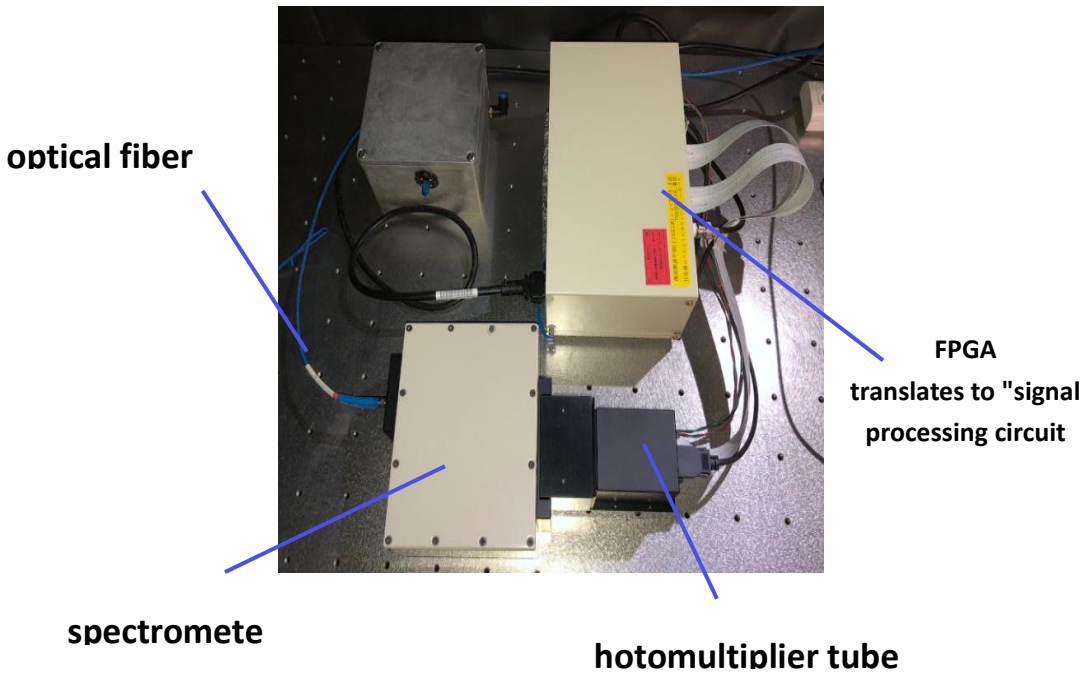

Fig3.1 configuration of the measurement system

Within this cycle, a pivotal component is the 32-channel photon counting photomultiplier tube (PMT). By incorporating a diffraction grating (Hamamatsu Photonics A10766-017-01) and a 32-channel photon-counting PMT (Hamamatsu Photonics H12211-20), we have constructed a high-speed wavelength-dispersive IBIL photon-counting detector. This apparatus is capable of measuring IBIL signals ranging from 320-750 nm within the irradiated area of a focused beam, thereby achieving high-sensitivity measurements across multiple wavelengths, with the data recorded in a photon-counting format.

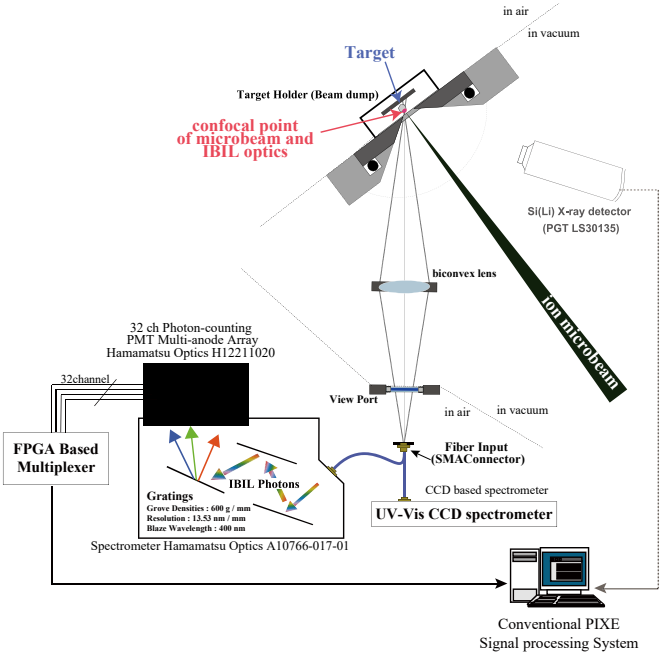

Fig3.2 Conceptual diagram of the IBIL microscopy optical system and multi-wavelength simultaneous spectrometer

To handle signals under a standard Analog-to-Digital Converter (ADC), we treated the 32-channel PMT photon-counting pulses in an analog format. We divided a 10V voltage into 32 distinct levels, assigning a unique voltage level to each channel. When a photon is detected in a channel, it is converted into the corresponding voltage, subsequently fed into the FPGA circuit for counting. By combining this data with the scanning location of the microbeam, we can realize wavelength-resolved imaging.

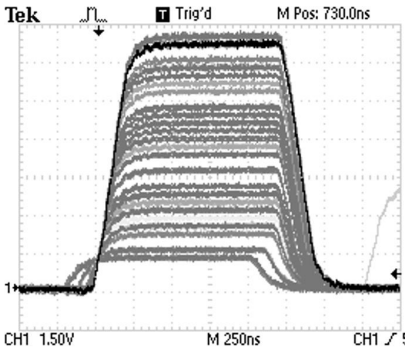

Fig3.3 Difference in peak values for each channel (maximum 10 V)

Prior to embarking on formal experiments, we subjected our entire system to tests using LED lights of varying wavelengths. We tested simulated inputs from blue, green, and multichannel LEDs, to ensure the system's functionality and accuracy in counting. Upon validation of photon counts across all channels, we conducted tests on the actual device, thereby confirming its precision and stability in real-worldapplications.

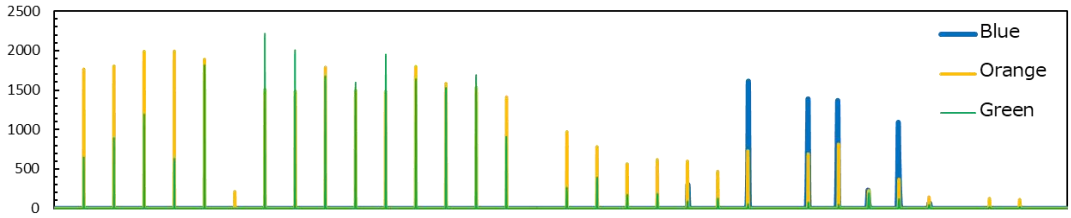

Fig3.4 MCA Output Graph

3.2experimental procedure

Our research has been conducted at the Takasaki Advanced Radiation Research Institute, under the purview of the Quantum Science and Technology Research Organization. We capitalized on the 3 MV single-ended accelerator light ion microbeam line available at the facility, establishing an Induced Beam-Induced Luminescence (IBIL) analysis system.[10]

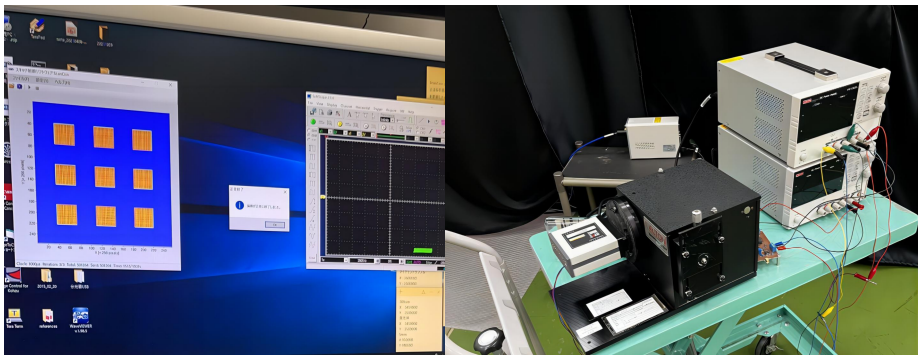

Fig3.6 PBW drawing in progress (left)Fig3.7 MPPC(right)

Prior to engaging in the Particle Beam Writing (PBW) process, we initiated an ion beam-induced luminescence analysis. This analysis allowed us to measure the luminescence output prior to irradiation, providing a vital baseline for subsequent processing.

Thereafter, we commenced with the PBW engraving. In the context of a focused proton beam processing system that could reach up to 3 MeV, we designated polymeric materials such as polymethylmethacrylate (PMMA) and photoresist materials, as well as organic samples[11], as targets for microfabrication. These materials were chosen due to their significant relevance in microfabrication applications and their well-characterized responses to ion irradiation.

Upon completion of the PBW engraving, we again performed IBIL analysis. By comparing the pre- and post-engraving luminescence, we were able to gain insights into the effects of the PBW process on these materials. This iterative process of luminescence analysis, PBW engraving, and post-engraving analysis was designed to maximize the information

we could glean from our experiment, allowing us to better understand the complex interactions between the ion beam and the target materials.

4Results and Analysis

4.1Result

Microfabrication through IBIL irradiation is a method where the results of the irradiation can only be first confirmed after post-irradiation processing. However, by using this method, we have demonstrated the possibility of monitoring the machining conditions during the irradiation process. After the experiments, we successfully obtained data, including

	ch	x	y
1	86	86	1
2	88	88	1
3	95	95	1
4	96	96	1

Table1 Data Format（"ch" translates to "channel", "x" stands for the horizontal coordinate, and "y" represents the vertical coordinate.）

energy levels (channels) and coordinate positions.

It was imperative to establish a meticulous counting mechanism. By employing a sophisticated Python algorithm, I systematically quantified the photons exhibiting identical energy magnitudes. Following the data acquisition, these results were methodically catalogued and presented in a structured tabular format for further analysis and interpretation. This approach not only ensured precision but also provided a foundation for subsequent research phases.Regarding the algorithm, please refer to the appendix.

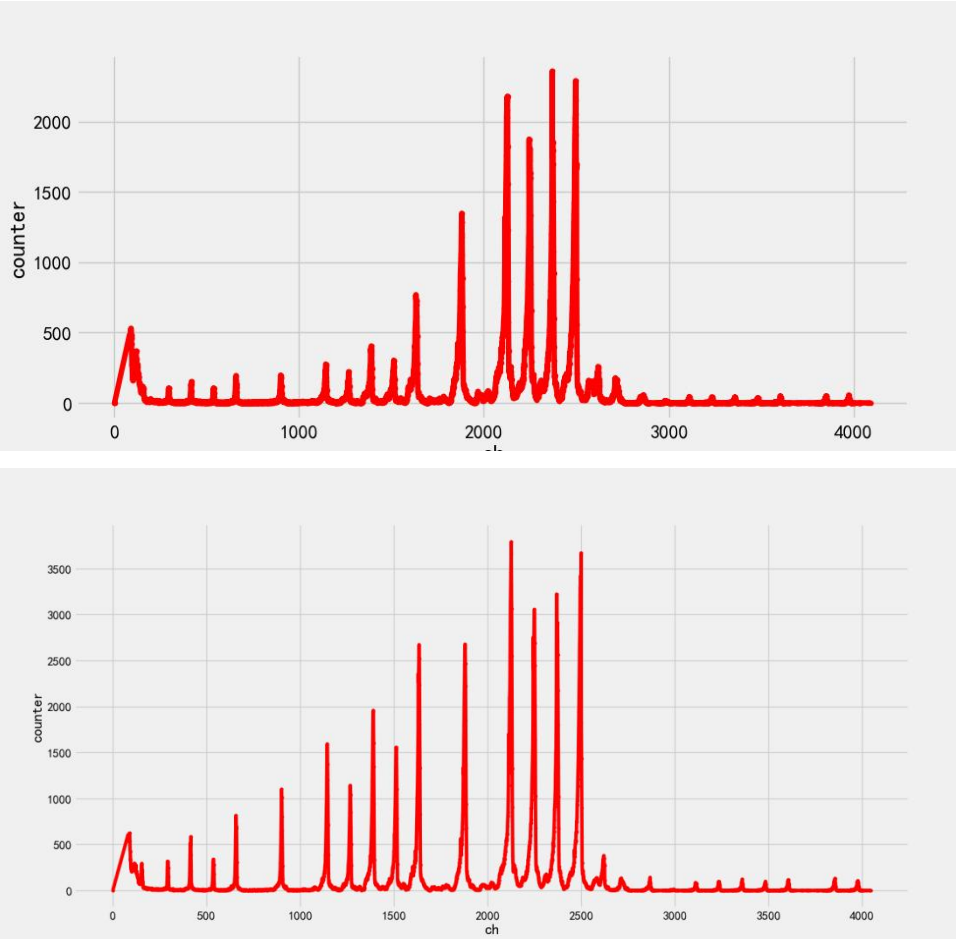

Fig4.1 IBIL output distribution in the irradiation area before PBW processing (top)
Fig4.2 IBIL output distribution in the irradiation area after PBW processing (bottom)

In the realm of proton beam processing, the physical and chemical responses between processed and unprocessed areas often exhibit significant disparities. To gain a deeper understanding of these differences and their implications for material properties, we crafted two sets of charts to scrutinize the energy distribution of ion beam-induced luminescence. Observably, post-pbw processing, there's a notable escalation in the photon count. However, the distribution and contour remain largely consistent. This preliminary insight suggests that pbw processing hasn't compromised the fundamental structure of the specimen.

4.2Analysis

4.2.1Increase in Photon Count

In the data curves of the table, it can be seen that under the same channel conditions, the number of photons before and after processing is basically consistent in terms of wavelength. However, there is a significant difference in the number of photons, with the count after irradiation being almost twice that before irradiation.

While the overall contours remain remarkably consistent, there is a noticeable increase in certain energy regions. The potential causes for this phenomenon can be delineated as follows:

1. Surface Alterations during Processing: The PBW processing could induce subtle changes in the material's surface microstructure. Such alterations might perturb the electronic band structure, potentially influencing the energy levels of emitted photons.

2. Changes in Crystalline Structure: PBW processing can result in transformations of the crystalline structure, manifesting as lattice distortions or the emergence of crystal boundaries. These structural changes could, in turn, modify the electronic band structure, which might further affect the energy of the photons.

3. on Beam-Induced Electron Excitation: During the PBW processing, interactions between the ion beam and the material can give rise to intricate physical and chemical effects. Among these, electron excitation

induced by the ion beam stands out. This process can lead to variations in the internal electronic energy levels of the material, subsequently impacting the photon energy.

4.2.2 Image Denoising Process

Subsequently, I integrated position information with energy distribution in graphical representation. By juxtaposing this with the previously obtained photon counts, Gaussian noise reduction was applied, resulting in the produced imagery. A comparative analysis of the preceding and subsequent images underscores the successful execution of the processing.

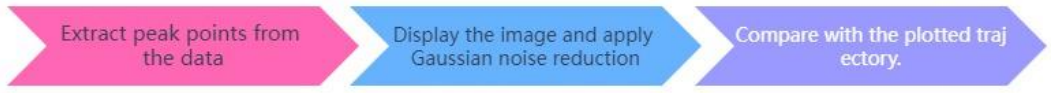

Fig4.3 Processing Procedure

After processing, we obtained the following image. The processing procedure can be clearly observed.

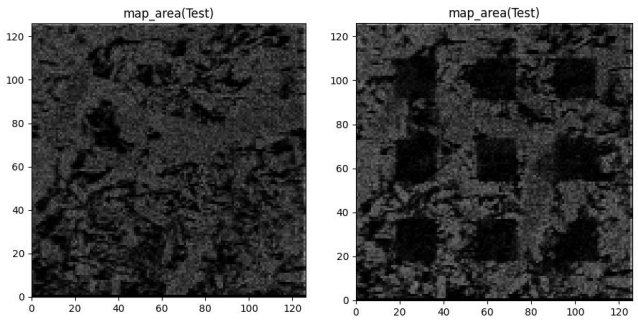

Fig4.4 Results after noise reduction processing: (left) before irradiation, (right) after irradiation.

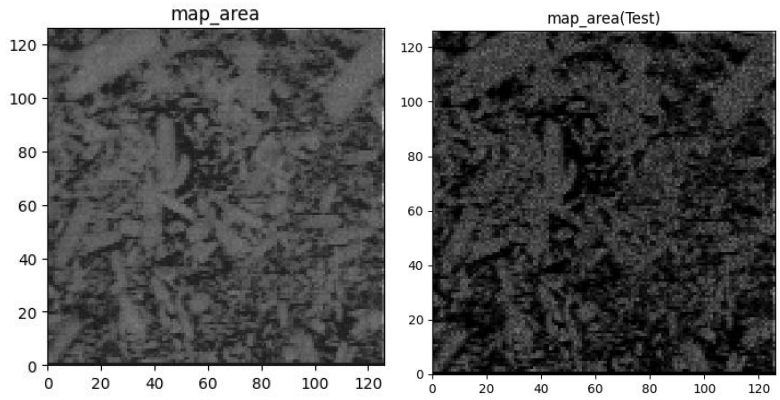

Fig4.5 Results beforer noise reduction processing (left)Results after noise reduction processing（right）

Firstly, a spectral analysis was conducted. Within the imaging domain, it's widely accepted that noise often presents as high-frequency components in an image's spectrum. By comparing the frequency distribution of the original image and the processed image, we noticed a significant suppression of these high-frequency components in the latter, indicating effective noise reduction.

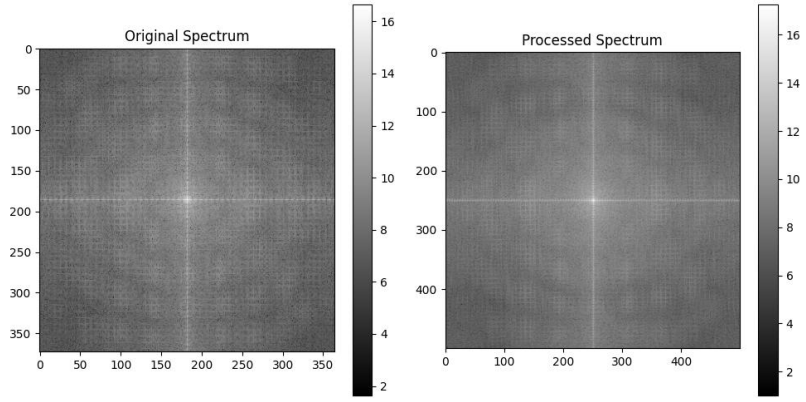

Fig4.5 Spectral graph before and after processing (left: before processing) (right: after processing)

From a statistical lens, the original and processed images are strikingly alike in their mean values, measuring at 125.32 and 125.60 respectively. Such nuanced differences intimate that, despite the denoising intervention, the foundational luminosity and chromatic framework of

the image have been retained. What's equally compelling, however, is the noticeable elevation in the standard deviation for the processed image, surging from 83.89 to 106.64. This suggests not just random variations but a deliberate enhancement in the contrast of the image. Moving on to the nuances of the distribution within the images, an intriguing trend surfaces. The transition from the original to the processed version revealed a substantial curbing of skewness. In essence, skewness gauges the tilt or asymmetry of data distribution. A higher skewness often denotes a pronounced extension on the distribution's right. Thus, with the diminished skewness in the processed image, we're witnessing a trend towards a more balanced and harmonious pixel spread, essentially making the image more even-toned. Equally noteworthy is the matter of kurtosis. Both images, in their statistical dance, exhibited a negative value for kurtosis, suggesting a more plateaued distribution in contrast to what one would expect from a regular bell curve. But it's the processed image that stands out further, presenting an even more tempered kurtosis, which essentially underscores a pixel distribution that's more evenly spread out and flattened

To further assess the differences between the two images, we calculated the Mean Square Error (MSE) and the Peak Signal-to-Noise Ratio (PSNR). The MSE quantifies the average squared pixel difference

between the two images and is given by:

$$\mathrm{MSE} = \frac{1}{MN} \sum_{i=0}^{M-1N-1} \sum_{j=0} [I(i,j) - K(i,j)]^2$$

Where I and K are the two images being compared, and M and N denote the dimensions of the images. Based on our computations, the MSE value stands at 80.66, reflecting that some differences were introduced during normalization.

The PSNR, on the other hand, evaluates the image quality based on the maximum possible pixel value and the MSE. It is defined as:

$$\mathrm{PSNR} = 20 \times \log_{10} \left(\frac{\mathrm{MAX}_I}{\sqrt{\mathrm{MSE}}} \right)$$

For 8-bit images, the maximum possible pixel value is 255. Our computed PSNR value is 29.06 dB, which is relatively low. This might suggest that the processing introduced some unintended changes or distortions.

In conclusion, while the processing effectively suppressed high-frequency noise in the spectrum, other changes might have been introduced when considering statistical properties and image quality indicators, such as PSNR.

5 Conclusion

Throughout this study, a system has been introduced that permits post-process observation of PBW (Proton Beam Writing) micromachining technology. One of the core methodologies behind this system is the implementation of IBIL analysis, which provides the capacity to evaluate morphological changes within the irradiated regions. This capability offers profound insights into the intricacies of the PBW process, thereby enhancing our understanding and precision.

A pivotal advancement heralded by this research is the development of a spectrometer capable of photon counting. This technology not only permits the simultaneous realization of IBIL spectroscopy and imaging but also paves the way for a comprehensive understanding of the intricate dynamics during PBW processing. The potential this dual capability offers is immense, potentially revolutionizing how we approach PBW micromachining.

Further investigation utilizing organic material samples highlighted the prospective advantages of IBIL information. Through IBIL's insights, there is a suggested potential for real-time monitoring of the machining status during irradiation. This real-time insight could be a game-changer, allowing for instantaneous modifications, ensuring the precision of the machining process, and minimizing errors.

In culmination, the technology proposed in this research presents a

promising avenue as a versatile technique for effortlessly evaluating micromachining areas. The fusion of PBW and IBIL technologies is expected to pave the way for a new era of micromachining, where precision, real-time monitoring, and efficient evaluation are the norms. As we move forward, the successful integration of these technologies might very well set the standard for future micromachining endeavors.

6Appendix or Appendices

[1] 横山浩 and 秋永広之, 電子線リソグラフィ教本,オーム社, 第 1 版. 2007.
[2] M. Kashiwagi, Y. Hoshi, and N. H. V Corporation, “電子線照射装置の技術とその利用,” pp. 50–57, 2012.
[3] W. Kada et al., Nucl. Instr. and Meth. Sec. B., 348, pp.218-222, (2015).
[4] R. K. Parajuli et al,.Jpn. Appl. Phys. 55, p. 06GD01, (2016).
[5] H. Kraus et al., Nano Letters, 17(5), pp. 2865-2870(2016).
[6] M. Haruyama et al., Key Eng. Mat.., 790, pp. 48-54, (2018).
[7] Hitachi High Technologies, “Focused Ion Beam (FIB): Principle Explanation.” [Online]. Available:https://www.hitachi-hightech.com/jp/science/technical/tech/microscopes/focused-ion-beam-systems/descriptions/
[8] 三浦聡, “修士論文 高分子材料を用いたマッハツェンダー導波路型光スイッチに関する 研究,” 群馬大学大学院理工学府理工学専攻電子情報･数理教育プログラム理工学専攻電 子情報･数理教育プログラム, 2018.
[9] W. Kada et al., Nucl. Instr. and Meth. Sec. B., 406, pp.124-129, (2017).
[10]Sync 研究室 群馬大学 鈴木孝明.” [Online]. Available: https://mems.mst.st.gunma-u.ac.jp/
[11] 小林潤也, 光インターコネクション入門,三松株式会社. 2010

7.References or Bibliography

7.1Preliminary Data Filtering

```
import sys
```

```
import os

import struct
import datetime
import pandas as pd
import numpy as np
import pandas as pd

class PIXEAnaData:
    """Process experimental data for PIXEDAQ"""

    def __init__(self):
        self.dose = float
        self.total = int
        self.width = float
        self.height = float
        self.MAX_CHANNEL_SIZE = int

        #生のリスト保存のデータ
        self.list_data = []
        #生のデータフレーム
        self.X=pd.DataFrame

        #エラーを削除したデータ
        self.X_normal=pd.DataFrame

        #エラーのデータ
        self.X_kick=pd.DataFrame

        # 完成品のデータ
        self.df=pd.DataFrame

        # スペクトルデータ
        self.spectrum=np.array



    def load_data_file(self, filenamePIXE):
        """Load a PIXEAna file"""
        #filename

        def get_last_index(data):
            """Get last index of event data"""
```

```
        last_index = len(data) - 2
        while (data[last_index] != (0, 0, 0) and
               data[last_index + 1] != (0, 0, 1)):
            last_index -= 1

        return last_index


    #ファイルのロード。 'r'：読み込み用で開きます。 'b'：バイナリモードで開きます。
    with open(filenamePIXE, "rb") as file:
        bin_data = [event for event
                    in struct.iter_unpack("HHH", file.read())]
    if bin_data[0] != (0, 0, 0xffff):
        sys.exit("Wrong type data file!")

    last_index = get_last_index(bin_data)

    #dose = bin_data[last_index + 5][0] / 10.0
    #total_dose = self.dose + dose

    #width = bin_data[last_index + 3][0]
    #height = bin_data[last_index + 3][1]
    #if total_dose > 0.0:
    #    self.width = (self.dose * self.width + dose * width) / total_dose
    #    self.height = (self.dose * self.height +
    #                   dose * height) / total_dose
    #else:
    #    self.width = width
    #    self.height = height

    #self.dose = total_dose
    #self.total += last_index - 1

    self.list_data.extend(bin_data[1:last_index])


#def sort 部分
def sort_list(self, ch_roi_start=0, ch_roi_end=4095,
              x_roi_start=0, x_roi_end=127,
              y_roi_start=0, y_roi_end=127,
              ch_size=4096, x_size=128, y_size=128):

    """Sort list"""
```

```
        self.MAX_CHANNEL_SIZE=ch_size

        self.X=np.array(self.list_data).reshape(-1, 3)
        self.X = pd.DataFrame(self.X)

        self.X.rename(columns={0: 'x'}, inplace=True)
        self.X.rename(columns={1: 'y'}, inplace=True)
        self.X.rename(columns={2: 'ch'}, inplace=True)

        self.X["x"]=self.X["x"]*x_size // 0x1000
        self.X["y"]=self.X["y"] * y_size // 0x1000
        self.X["ch"]=self.X["ch"]*ch_size // 0x1000


        def normal_fun(row):
          if not row & 0x1000:
            return row
          else:
            return row*np.nan

        self.X_normal = self.X.copy()
        self.X_normal["ch"] = self.X["ch"].apply(normal_fun)
        self.X_normal=self.X_normal.dropna(how='any', axis=0).astype('int')

        def kick_fun(row):
          if row & 0x1000:
            return row
          else:
            return row*np.nan
        self.X_kick = self.X.copy()
        self.X_kick["ch"] = self.X["ch"].apply(kick_fun)
        self.X_kick=self.X_kick.dropna(how='any', axis=0).astype('int')


        #Extract events in ROI
         self.df=(self.X_normal[(ch_roi_start<=self.X_normal["ch"])&(self.X_normal["ch"]<=ch_roi_
end)&
                                (x_roi_start<= self.X_normal["x"])&(self.X_normal["x"]<=x_roi_end)&
                                (y_roi_start<= self.X_normal["y"])&(self.X_normal["y"]<=y_roi_end)])

        # カウントを集計してスペクトルデータにする。
        self.spectrum,_=np.histogram(self.df['ch'].values, bins=self.MAX_CHANNEL_SIZE, range=(0,
self.MAX_CHANNEL_SIZE), density=False)
```

Image Display

```
from matplotlib import pyplot as plt

def mapfunc(PIXEAnaData):

  x=PIXEAnaData.df['x'].values
  y=PIXEAnaData.df['y'].values

  xedge = np.arange(max(x))
  yedge = np.arange(max(y))

  H1, xedges, yedges = np.histogram2d(x, y, bins=(xedge, yedge))

  fig = plt.figure(figsize=(5, 5))
  ax = fig.add_subplot(111, title='map_area')
  plt.imshow(H1.T,cmap='Greys_r' ,interpolation='nearest', origin='lower',
             extent=[xedges[0], xedges[-1], yedges[0], yedges[-1]])
  plt.show()

if __name__=="__main__":

  mapfunc(PIXEana)
```

Line Graph Drawing

```
import numpy as np
import pandas as pd
import matplotlib.pyplot as plt

plt.style.use("fivethirtyeight")
plt.rcParams['font.sans-serif'] = ['KaiTi', 'SimHei', 'FangSong']

data = pd.read_csv("D:/desktop/tset/test 2.0/新建文件夹/after-irradiation3H.csv")
dataCH = data['ch'].values.tolist()

SetCH = set(dataCH)
ListCH = list(SetCH)

if len(ListCH) > 0:
    num = 0
    index = 0
    yy = []
```

```
    for j in dataCH:
        if j == ListCH[index]:
            num += 1
        else:
            yy.append(num)
            index += 1
            num = 1
            if index >= len(ListCH):
                break
    yy.append(num)

    # 确保 ListCH 和 yy 的长度相同
    if len(ListCH) > len(yy):
        ListCH = ListCH[:len(yy)]

    plt.figure(figsize=(25, 15))
    plt.plot(ListCH, yy, 'r.-')
    plt.ylabel('counter')
    plt.xlabel('ch')
    plt.show()
else:
    print("No unique 'ch' values found in the data.")
```

Light Filtration

```
import numpy as np
import pandas as pd
import matplotlib.pyplot as plt

PIXEAna = pd.read_csv("D:/desktop/tset/test 2.0/新建文件夹/after-irradiation3H.csv")
x = PIXEAna['x']
y = PIXEAna['y']
xedge = np.arange(max(x))
yedge = np.arange(max(y))

H1, xedges, yedges = np.histogram2d(x, y, bins=(xedge, yedge))
# print(H1)
# print(xedges)
# print(yedges)
fig = plt.figure(figsize=(5, 5))
ax = fig.add_subplot(111, title='map_area(Test)')
```

```
plt.imshow(H1.T, cmap='Greys_r', interpolation='nearest', origin='lower',
           extent=[xedges[0], xedges[-1], yedges[0], yedges[-1]])

minn = int(input("CHmin(0-4095)："))
maxx = int(input("CHmax0-4095)："))
realmin = (minn/4095)*100
realmax = (maxx/4095)*100
plt.clim(realmin,realmax)
# plt.clim(9, 19)
plt.show()
```

normalization

```
import cv2
import numpy as np

# 读取原始图像和处理后的图像
original = cv2.imread('D:/desktop/tset/picture/irradiation/2/before-irradiation2H.png',
cv2.IMREAD_GRAYSCALE)
processed = cv2.imread('D:/desktop/tset/picture/irradiation/2/before.png',
cv2.IMREAD_GRAYSCALE)

# 确保两张图像的尺寸一致
if original.shape != processed.shape:
    processed = cv2.resize(processed, (original.shape[1], original.shape[0]))

# 计算 MSE
mse = np.sum((original - processed) ** 2) / float(original.shape[0] * original.shape[1])


# 计算 PSNR
if mse == 0:
    psnr = 100
else:
    max_pixel = 255.0
    psnr = 20 * np.log10(max_pixel / np.sqrt(mse))

print(f"MSE: {mse}")
print(f"PSNR: {psnr}")
```

frequency spectrogram

```
import cv2
import numpy as np
import matplotlib.pyplot as plt

def compute_magnitude_spectrum(image):
    # 进行傅立叶变换并得到其幅度频谱
    f = np.fft.fft2(image)
    fshift = np.fft.fftshift(f)
    magnitude_spectrum = np.log(np.abs(fshift) + 1)
    return magnitude_spectrum

def display_spectrum(image, title):
    magnitude_spectrum = compute_magnitude_spectrum(image)
    plt.imshow(magnitude_spectrum, cmap='gray')
    plt.title(title)
    plt.colorbar()

def main():
    # 加载图像
        original = cv2.imread('D:/desktop/tset/picture/irradiation/2/before-irradiation2H.png',
cv2.IMREAD_GRAYSCALE)
                processed = cv2.imread('D:/desktop/tset/picture/irradiation/2/before.png',
cv2.IMREAD_GRAYSCALE)

    # 显示频谱
    plt.figure(figsize=(10, 5))

    plt.subplot(1, 2, 1)
    display_spectrum(original, 'Original Spectrum')

    plt.subplot(1, 2, 2)
    display_spectrum(processed, 'Processed Spectrum')

    plt.tight_layout()
    plt.show()

if __name__ == '__main__':
    main()
```

count

```
import cv2
import numpy as np
from scipy.stats import skew, kurtosis

def image_statistics(img):
    # 计算均值、标准差、偏度和峰度
    mean = np.mean(img)
    std_dev = np.std(img)
    skw = skew(img.ravel())
    kurt = kurtosis(img.ravel())

    return mean, std_dev, skw, kurt

# 读取原始图像和处理后的图像
img1 = cv2.imread('D:/desktop/tset/picture/irradiation/2/before-irradiation2H.png', 0)  # 0 表示读取为灰度图像
img2 = cv2.imread('D:/desktop/tset/picture/irradiation/2/before.png', 0)

# 计算统计数据
stats1 = image_statistics(img1)
stats2 = image_statistics(img2)

print("Original Image:")
print(f"Mean: {stats1[0]}, Std Dev: {stats1[1]}, Skewness: {stats1[2]}, Kurtosis: {stats1[3]}")

print("\nProcessed Image:")
print(f"Mean: {stats2[0]}, Std Dev: {stats2[1]}, Skewness: {stats2[2]}, Kurtosis: {stats2[3]}")
```